We are IntechOpen,
the world's leading publisher of
Open Access books
Built by scientists, for scientists

6,900
Open access books available

185,000
International authors and editors

200M
Downloads

154
Countries delivered to

Our authors are among the

TOP 1%
most cited scientists

12.2%
Contributors from top 500 universities

CLARIVATE ANALYTICS

BOOK CITATION INDEX

INDEXED

WEB OF SCIENCE™

Selection of our books indexed in the Book Citation Index
in Web of Science™ Core Collection (BKCI)

Interested in publishing with us?
Contact book.department@intechopen.com

Numbers displayed above are based on latest data collected.
For more information visit www.intechopen.com

Coding, Modulation, and Detection for Power-Efficient Low-Complexity Receivers in Impulse-Radio Ultra-Wideband Transmission Systems

Andreas Schenk and Robert F.H. Fischer

Additional information is available at the end of the chapter

http://dx.doi.org/10.5772/53261

1. Introduction

Impulse-radio ultra-wideband (IR-UWB) is a promising transmission scheme, especially for short-range low-data-rate communications, as, e.g., in wireless-sensor networks. One of the main reasons for this is its potential to employ noncoherent, hence low-complexity, receivers even in dense multipath propagation scenarios, where channel estimation required for coherent detection would be overly complex due to the large signal bandwidth and hence rich multipath propagation [23].

Differential pulse-amplitude-modulated IR-UWB in combination with autocorrelation-based detection constitutes an attractive variant of noncoherent detection schemes [11]. The inherent loss in performance of traditional noncoherent autocorrelation-based differential detection (DD), as compared to coherent detection based on explicit channel estimation, can be alleviated by advanced autocorrelation-based detection schemes operating on the output of an extended autocorrelation receiver (ACR). This ACR delivers correlation coefficients of symbols separated by several symbol durations. In this context, block-based detection schemes, which partition the receive symbol stream into (possibly overlapping) blocks and thus process multiple symbols jointly, have proven to enable power-efficient, yet low-complexity detection in both uncoded and coded IR-UWB transmission systems [3, 6, 11, 12, 15–18].

In this chapter, a comprehensive review of block-based detection schemes is presented. Starting with an exposition of the operation in uncoded schemes, we discuss the generation of soft output, required in coded IR-UWB systems employing autocorrelation-based detection. For the design of such systems, an information theoretic performance analysis of IR-UWB transmission with autocorrelation-based detection delivers design rules for coded IR-UWB systems. In particular, optimum rates for the applied channel code are derived, which improve the overall power efficiency (i.e., required signal-to-noise ratio to guarantee a desired error rate) of the system. The chapter concludes with a brief summary.
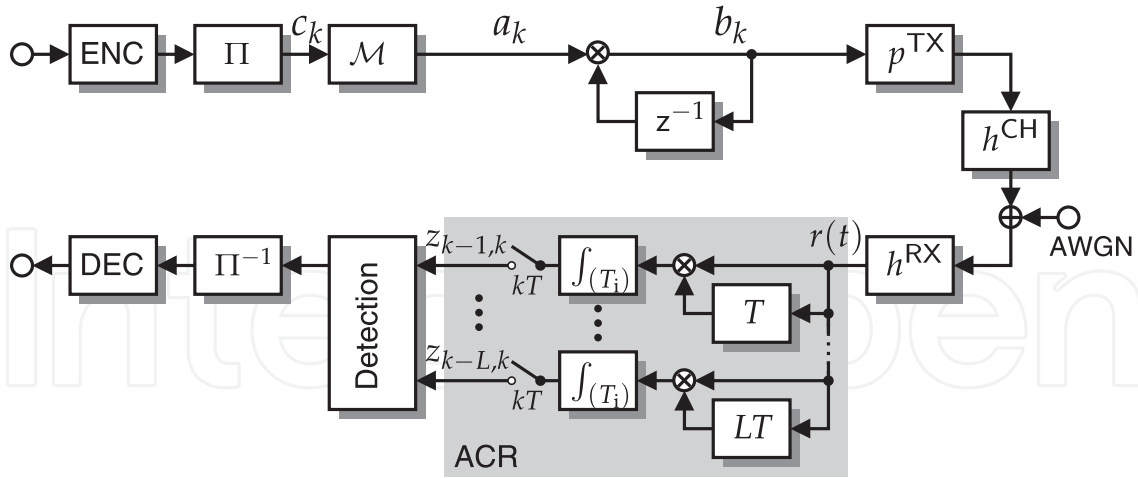
2. IR-UWB system model with autocorrelation-based detection

2.1. IR-UWB system model

Throughout this chapter binary pulse-amplitude-modulated IR-UWB transmission in combination with bit-interleaved coded modulation (BICM), as shown in Fig. 1, is considered. Avoiding up-/downconversion due to operation at a carrier frequency, transmission takes place in the baseband; hence, all signals are real valued. The sequence of information bits (assumed to be equiprobable and independent, i.e., with maximum entropy) is encoded with a channel code of rate R_c. After symbolwise mapping from (interleaved) codeword bits c_k to binary information symbols $a_k \in \{\pm 1\}$, differential encoding is performed, yielding the transmit symbols $b_k \in \{\pm 1\}$, where $b_k = b_{k-1}a_k$ and $b_0 = 1$. The IR-UWB receive signal, after propagation through an UWB multipath channel, is given by [23]

$$r(t) = \sum_{k=0}^{+\infty} b_k p(t - kT) + n(t) \tag{1}$$

where T is the symbol duration and $p(t)$ denotes the overall receive pulse shape, resulting from the convolution of transmit (TX) pulse, receive (RX) filter, and channel (CH) impulse response; its energy is normalized to one, thus, the energy per information symbol[1] is given as $E_s = 1$. We assume the channel to remain constant within one codeword. $n(t)$ results from white Gaussian noise of two-sided power-spectral density $N_0/2$ passed through the RX filter. To preclude inter-symbol interference, the symbol duration T is chosen sufficiently large, such that each pulse has decayed before the next pulse is received. For clarity, we do not explicitly consider the typically applied frame structure used for time-hopping and code-division multiple access, as it can be averaged out prior to further receive signal processing [6].

Figure 1. System model of coded IR-UWB transmission with autocorrelation-based detection.

For convenient representation and in view of an all-digital implementation of the receiver, we define the sampled receive signal of the kth symbol interval as $\bar{r}_k = [r(kT), r(kT + T_s), \ldots, r(kT + (N_s - 1)T_s)]^\mathsf{T}$, where $N_s = f_s T$ is the number of samples per symbol interval, and $f_s = 1/T_s$ is the sampling rate (greater than or equal to the Nyquist rate). With respective

---

[1] For long bursts, the energy for the reference symbol may be neglected.

definitions for the end-to-end impulse and the noise, assuming no inter-symbol interference, we compactly write

$$\bar{r}_k = b_k \bar{p} + \bar{n}_k \, . \tag{2}$$

The noise components in $\bar{n}_k$ are modeled as uncorrelated Gaussian random variables with variance $\sigma_n^2 = f_s N_0 / 2$, which is the case for a square-root Nyquist low-pass receiver front-end filter with two-sided bandwidth f_s.

2.2. Autocorrelation-based detection

Autocorrelation-based noncoherent detection of IR-UWB, cf., e.g., [2, 3, 6, 9, 15], requires to compute the correlation of the current symbol with up to L preceeding symbols, as shown in Fig. 1. Significant gains are achieved by adopting the integration interval to the channel characteristics at hand [23], i.e., choosing $T_i < T$ in the order of the expected channel delay spread. Simplified, larger T_i lead to decreased performance, but become inevitable in case of only coarse synchronization or insufficient knowledge of the channel characteristics[2]. Defining the time-bandwidth product $N = f_s T_i$ and r_k as the part of $\bar{r}_k$ relevant for the ACR integration, i.e., (typically the first) N successive components out of N_s, in an digital implementation we have, for $l = 1, \ldots, L$,

$$z_{k-l,k} = r_{k-l}^\mathsf{T} r_k \, . \tag{3}$$

The correlation coefficients serve as input for various detection schemes, cf., Sec. 3 and [3, 6, 9, 10, 12, 15, 23]. E.g., symbolwise differential detection (DD) utilizes only the correlation coefficient of the current symbol and its predecessor, i.e., $L = 1$, and, since $b_{k-1} b_k = a_k$, the decision rule for the information symbols reads $a_k^{\mathsf{DD}} = \mathrm{sign}(z_{k-1,k})$.

We explicitly point out the major drawback of an autocorrelation-based receiver, namely the required accurate analog delay lines in an analog implementation, or the large sampling rate[3] in an all-digital implementation. Especially approaches based on the principle of compressed sensing (CS) promise to circumvent these problems [14, 24]. These approaches avoid sampling the receive signal at the (possibly prohibitively) large Nyquist rate by taking fewer measurements in a different domain (e.g., frequency or some transform domain). In [14] it has been shown, that a CS-front-end can readily be applied prior to an ACR, i.e., via direct correlation of the measurements, thus also avoiding the need for computationally complex CS-reconstruction algorithms. In combination with autocorrelation-based DD the inherent loss in performance of CS/ACR-based detection is proportional only to the square root of the compression ratio (number of measurements over N_s) [14].

2.3. Equivalent discrete-time system model

Based on the all-digital implementation, we introduce an equivalent discrete-time system model of ACR-based detection. The ACR-output can be written as

$$z_{k-l,k} = E_i x_{k-l,k} + \eta_{k-l,l} \tag{4}$$

---

[2] A typical setting for realistic IR-UWB scenarios, e.g., modelled by the IEEE channel models [7, 8] is $T_i = 33$ ns, whereas $T = 75$ ns to avoid inter-symbol interference. With $f_s = 12$ GHz, we have $N_s = 900$ and $N \approx 400$ [23].

[3] With the advance in micro electronics, one can expect that an all-digital implementation becomes realistic within no later than the next decade.

where $E_i = \boldsymbol{p}^\mathsf{T}\boldsymbol{p}$ denotes the captured pulse energy. It is composed of the phase transition from b_{k-1} to b_k, i.e., $x_{k-l,k} = b_{k-l}b_k$, and "information × noise" and "noise × noise" terms, summarized in the equivalent noise term

$$\eta_{k-l,l} = b_{k-l}\boldsymbol{p}^\mathsf{T}\boldsymbol{n}_k + b_k\boldsymbol{n}_{k-l}^\mathsf{T}\boldsymbol{p} + \boldsymbol{n}_{k-l}^\mathsf{T}\boldsymbol{n}_k \ . \tag{5}$$

A detailed analysis of the components of the equivalent noise term in (5) shows that already for moderate time-bandwidth products N it is reasonable to approximate the respective terms as uncorrelated Gaussian random variables [9, 10, 14]. In particular, the "information × noise" terms are zero-mean with variance σ_n^2, and the "noise × noise" term, as the sum of N products of independent Gaussian random variables, is zero-mean with variance $N(\sigma_n^2)^2$. Consequently, $\eta_{k-l,k}$ may be modeled as a zero-mean Gaussian random variable with variance $\sigma_\eta^2 = 2\sigma_n^2 + N(\sigma_n^2)^2$. Since each $\eta_{k-l,k}$ results from the multipication of different parts of noise and symbols, the equivalent noise samples at different time instances and ACR branches are uncorrelated.

This approximation is only valid under the following prerequisites, which typically are fulfilled in common IR-UWB systems: i) the symbol duration is chosen sufficiently large, such that no inter-symbol interference is present, ii) the integration interval of the ACR and the time-bandwidth product N are chosen sufficiently large, such that the Gaussian approximation holds, iii) the receiver front-end filter is a square-root Nyquist low-pass with two-sided bandwidth f_s to avoid correlations of the noise samples, and iv) the channel remains constant over the block of at least $L + 1$ symbols. We emphasize that this model not only enables the subsequent information theoretic analysis of ACR-based detection of IR-UWB, but also serves as a tool for efficient numerical simulations of the IR-UWB transmission chain.

3. Advanced detection schemes for IR-UWB

3.1. Multiple-symbol differential detection

One of the most powerful detection schemes is based on the principle of multiple-symbol differential detection (MSDD), cf., [1] and its modifications for IR-UWB detection [3, 6, 15]. In MSDD the stream of receive symbols is decomposed into blocks of $L + 1$ symbols (note that the blocks have to overlap by at least one symbol), and for each block the blockwise-optimal sequence of L information symbols is decided jointly based on the correlation coefficients corresponding to this block. The decision metric given a hypothesis of information symbols grouped into a vector $\tilde{\boldsymbol{a}}$ and the corresponding hypothesis of the ACR output $\tilde{\boldsymbol{x}}$, reads

$$\Lambda(\tilde{\boldsymbol{a}}) = \sum_{k=1}^{L} \left(\sum_{l=0}^{k-1} \left(|z_{l,k}| - \tilde{x}_{l,k} z_{l,k} \right) \right) \ . \tag{6}$$

The blockwise-optimal sequence $\boldsymbol{a}^{\mathsf{MSDD}}$ of hard-output MSDD is given as the sequence with minimum decision metric.

To fully exploit the benefits of channel coding, reliability information on the estimated codeword bits should be delivered to the subsequent channel decoder, i.e., so-called soft-output MSDD (SO-MSDD) should be performed. Sticking to the so-called max-log

approximation, in terms of log-likelihood ratios (LLRs) reliability information corresponds to the (scaled) difference of the decision metric of the optimum sequence [12], i.e.,

$$\Lambda^{\mathsf{MSDD}} = \Lambda(\boldsymbol{a}^{\mathsf{MSDD}}) = \min_{\tilde{\boldsymbol{a}} \in \{\pm 1\}^L} \Lambda(\tilde{\boldsymbol{a}}) \tag{7}$$

and the decision metric of the corresponding counter hypothesis, i.e., the minimum metric with the restriction $\tilde{a}_k = -a_k^{\mathsf{MSDD}}$, i.e., for $k = 1, \ldots, L$,

$$\Lambda_k^{\overline{\mathsf{MSDD}}} = \min_{\tilde{\boldsymbol{a}} \in \{\pm 1\}^L, \, \tilde{a}_k = -a_k^{\mathsf{MSDD}}} \Lambda(\tilde{\boldsymbol{a}}) \, . \tag{8}$$

Finally, the reliablitiy of the kth symbol/codeword bit is proportional to

$$\mathsf{LLR}_k \sim a_k^{\mathsf{MSDD}} \left(\Lambda_k^{\overline{\mathsf{MSDD}}} - \Lambda^{\mathsf{MSDD}} \right) \, . \tag{9}$$

In the case of SO-DD ($L = 1$), the LLRs are directly given as the (scaled) ACR output, i.e., $\mathsf{LLR}_k^{\mathsf{DD}} \sim z_{k-1,k}$ [12].

Utilizing the triangular structure of the decision metric, an efficient solution to the MSDD search problem (7) is obtained by employing the sphere decoder algorithm [6, 18, 19]. In the case of SO-MSDD, incorporating modifications in the sphere decoder algorithm proposed for efficient soft-output detection in multi-antenna systems [21], the $L + 1$ search problems per block, (7) and (8), can be solved in a single sphere decoder run per block using the single-tree-search soft-output sphere decoder [12, 21]. Thus, SO-MSDD can be realized at only moderate complexity increase compared to hard-output MSDD.

3.2. Decision-feedback differential detection

A closely-related detection scheme is blockwise decision-feedback differential detection (DF-DD), cf., [5] and its modifications for IR-UWB detection [15], which decides the symbols within each block in a successive manner taking into account the feedback from already decided symbols within the block. The blockwise processing of the receive signal enables to optimize the decision order, such that in each step the most reliable symbol is decided next, resulting in almost the performance of MSDD at lower and in particular constant complexity.

Briefly sketched, following [15] and focusing on the first block, with $\hat{k}_0 = 0$, $b_0^{\mathsf{DF\text{-}DD}} = 1$, the optimized decision order and the estimates are given by

$$\hat{k}_i = \operatorname*{argmax}_{k \in \{1, \ldots, L\} / \{\hat{k}_1, \ldots, \hat{k}_{i-1}\}} \left| \sum_{l=0}^{i-1} z_{\hat{k}_l, k} \, b_{\hat{k}_l}^{\mathsf{DF\text{-}DD}} \right| \tag{10}$$

$$b_{\hat{k}_i}^{\mathsf{DF\text{-}DD}} = \operatorname{sign} \sum_{l=0}^{i-1} z_{\hat{k}_l, \hat{k}_i} \, b_{\hat{k}_l}^{\mathsf{DF\text{-}DD}} \, . \tag{11}$$

Basically, the optimized decision order forces reliable decisions for the first decided symbols, which then strongly influence the upcoming decisions. In contrast to the related detection scheme BLAST in multiple-antenna systems, sorting is done per block based on the actual receive symbols and previous decisions, rather than on the channel realization.

3.3. Low-complexity soft-output detection via combining multiple observations

The blockwise processing of the receive symbol stream enables a further possibility to improve the performance without increase of the maximum delay of the ACR [17]. This method utilizes an overlapping block-structure. Since multiple blocks thus contain the same symbol, processing of each block delivers (possibly different) beliefs on the same symbol, i.e., multiple observations are available. Suitably combining the observations obtained from processing of each block, results in a (possibly more reliable) final decision. Depending on the applied blockwise decision scheme (here SO-MSDD and DF-DD are considered), there are different options how to combine multiple soft/hard observations to deliver a final hard and/or soft decision for the respective symbol [17]. The most interesting option is to combine multiple hard decisions, e.g., obtained from DF-DD, of the same symbol to form a single soft decision. This method can be implemented by using the sum of the individual hard-decisions as (quantized and scaled) "soft-output"; it preserves the low complexity of blockwise DF-DD, yet enables to exploit the additional gain of soft- vs. hard-decision channel decoding.

3.4. Performance of advanced detection schemes for uncoded IR-UWB transmission

In Fig. 2 the presented ACR-based detection schemes are compared with respect to bit error rate of uncoded IR-UWB transmission and a time-bandwidth product of $N = 400$. This parameter setting is based on the reasoning in Footnote 2; the Gaussian approximation as described in Sec. 2.3 is employed assuming that the integration interval captures the entire pulse energy, i.e., $E_i = E_s$). It can be observed, that i) with increasing blocksize performance improves over traditional DD (the significant loss compared to coherent detection is mainly caused by the squared original noise variance σ_n^2 in the equivalent noise variance σ_η^2) and approaches coherent detection with perfect channel estimation, ii) DF-DD with optimized decision order (dashed lines) achieves almost the performance of MSDD (solid lines, exactly the same performance for $L = 2$ with minimum overlap, and iii) combining multiple observations obtained by introducing a maximum block-overlap, but using the same ACR front-end (right hand side of Fig. 2) leads to significant gains over traditional blockwise processing without overlapping blocks (left hand side of Fig. 2), for both soft-output MSDD and hard-output DF-DD (except for $L = 2$) as blockwise detection scheme. This gain comes at the cost of an increased computational complexity (roughly proportional to L).

4. Design rules for coded IR-UWB systems

Based on an information theoretic performance analysis of IR-UWB in combination with ACR-based detection [16], in this section design rules for coded IR-UWB transmission systems are derived and verified by means of numerical results employing convolutional codes.

4.1. Capacity of IR-UWB with MSDD

In contrast to coded modulation using multi-level codes [22], common IR-UWB systems adopt the conventional serial concatenation of coding and modulation at transmitter, and detection and decoding at receiver side, as shown in Fig. 1, i.e., restrain to the BICM philosophy. This approach offers increased flexibility and robustness in fading scenarios. The BICM capacity of the overall transmission chain composed of mapping, differential encoding, and ACR-based
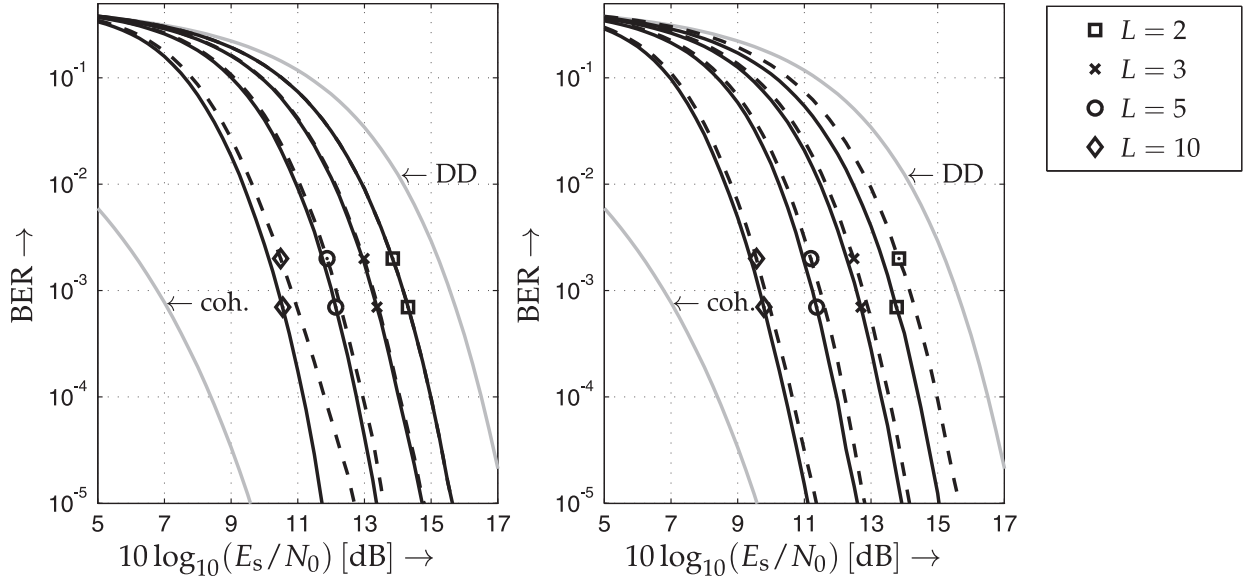
Figure 2. BER of uncoded BPSK IR-UWB transmission with autocorrelation-based detection with $L = 2$, 3, 5, and 10 (right to left). Solid: MSDD, dashed: DF-DD, left: processing of non-overlapping blocks, right: combining of multiple observations obtained by processing of maximum-overlapping blocks. Gaussian approximation with time-bandwidth product $N = 400$.

detection, is depicted in Fig. 3 (using the same parameter setup as in Sec. 3.4). Since an exact evaluation of the BICM capacity of the IR-UWB system at hand is overly complex, the equivalent discrete-time channel model and the Gaussian approximation, as derived in Sec. 2.3, have been applied [16]. Soft-output MSDD with $L = 2, 5$, and 10 (solid black), DF-DD with $L = 2$ and 5 (dashed black), and soft- and hard-output DD (solid gray/dashed gray) are shown; for comparison the capacity of BPSK with coherent detection is included.

In line with the BER results, the ACR operation causes a significant gap compared to coherent detection; the capacity improves with increasing blocksize. As expected for noncoherent detection schemes, cf., e.g., [20], the capacity curves of IR-UWB with ACR-based detection plotted vs. E_b/N_0, with E_b denoting the energy per information bit, have a C-like shape. Thus, as opposed to coherent detection, the minimum ratio E_b/N_0, which still guarantees reliable transmission, is obtained at non-zero rates (indicated with markers). At the operating point of minimum E_b/N_0 and optimum rate, both options, decreasing and increasing the code rate, lead to operating points which do not allow reliable transmission. Consequently, as known from other noncoherent detection schemes [20], also in realistic BICM IR-UWB systems the code rate should be carefully selected. Especially for increasing L this minimum gets more and more pronounced, and higher code rates should be favored compared to the probably more common choice of $R_c = 0.5$ [4]. In all cases, the optimum rate for the hard-output schemes DD and DF-DD is larger than the respective optimum rate of soft-output MSDD.

These effects are also observed for noncoherent detection (energy detection) of pulse-position modulation [20]. However, in this case already the application of BICM in combination with coherent detection leads to optimum operating points at non-zero code rates [13].
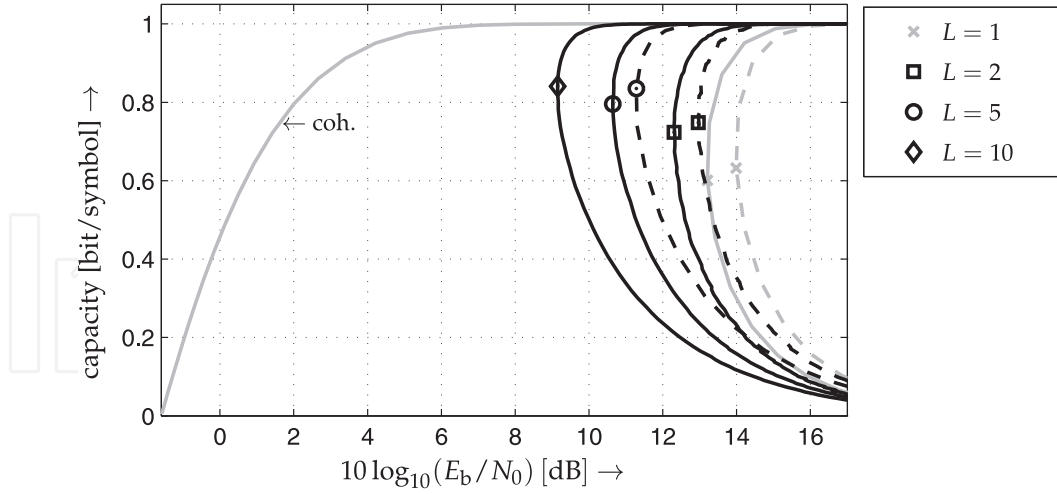
Figure 3. Capacity of BICM BPSK IR-UWB for soft/hard-output DD (solid gray/dashed gray), soft-output MSDD with $L = 2, 5$, and 10 (solid black), and DF-DD with $L = 2$ and 5 (dashed black). Gaussian approximation with time-bandwidth product $N = 400$.

In addition, a more detailed analysis shows that in non-fading scenarios an interleaver is not required for BICM IR-UWB [16].

4.2. Performance of advanced detection schemes for coded IR-UWB transmission

Finally, the design rules derived above are verified by means of numerical simulations. Fig. 4 depicts the BER of coded IR-UWB transmission using convolutional codes with optimized code rate compared to the default rate choice of $R_c = 0.5$. We apply the same channel model as in Sec. 3.4), and nonrecursively nonsystematically encoded maximum-free-distance convolutional codes with constraint length $\nu = 4$. For soft-output DD, the optimum rate
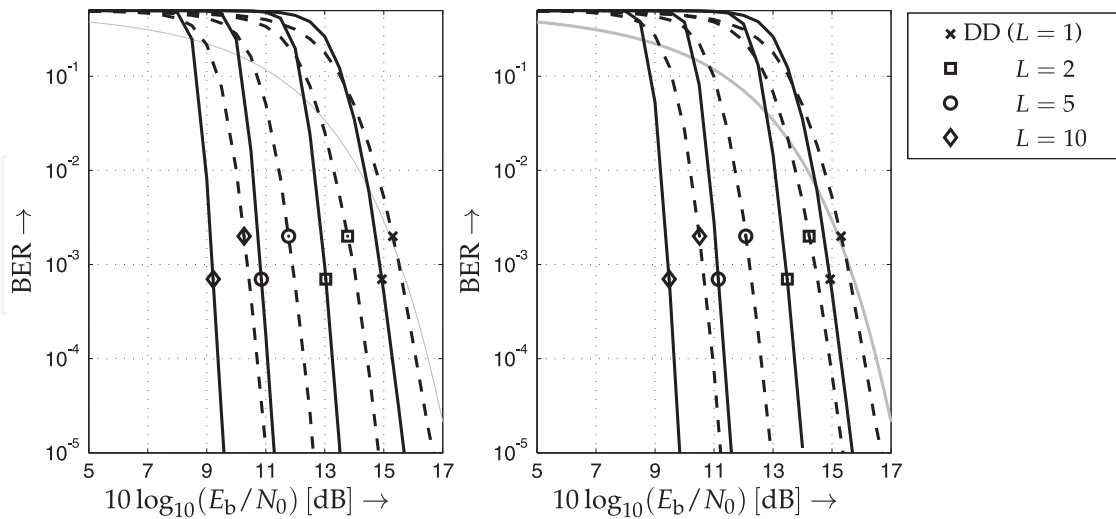
Figure 4. BER of convolutionally-coded BICM BPSK IR-UWB with autocorrelation-based detection with $L = 1, 2, 5$, and 10 (right to left). Solid: optimum code rate ($R_c = 2/3$ for DD with $L = 1$ and $R_c = 3/4$ for $L = 2, 5$ and 10), dashed: $R_c = 1/2$, gray: DD uncoded, left: soft-output MSDD, right: DF-DD, both using multiple-observations combining with maximum overlap. Gaussian approximation with time-bandwidth product $N = 400$.

is quantized to $R_c = 2/3$. Note that due to the increased decoder complexity of high-rate convolutional codes, for MSDD/DF-DD $R_c = 3/4$ is selected for all L, although higher rates are suggested by Fig. 3. ACR-based detection using soft-output MSDD (left) and DF-DD (right) with multiple observations combining is applied. It can clearly be observed that the performance is significantly improved with an optimized choice of the code rate, although the optimum code rates are larger than the default setting of $R_c = 0.5$ for all L—of course the relations are exactly opposite for coherent detection. As expected from the shape of the curves in Fig. 3, this effect is emphasized for larger blocksizes, yielding gains of almost 1 dB for $L = 10$ compared to $R_c = 0.5$.

Similar results are obtained for different coding schemes, such as LDPC codes with belief-propagation decoding [16], and also for coded IR-UWB pulse-position modulation in combination with energy detection.

5. Summary and conclusions

In this chapter we have presented a comprehensive review of coding, modulation, and detection for IR-UWB binary phase-shift keying. We conclude that noncoherent autocorrelation-based receivers in combination with blockwise detection constitute a power-efficient low-complexity reference for uncoded, as well as coded transmission. We derived and verified design rules for coded IR-UWB systems, in particular optimum code rates, which take into account the noncoherent detection at the receiver side.

Author details

Andreas Schenk
Lehrstuhl für Informationsübertragung, Friedrich-Alexander-Universität Erlangen-Nürnberg, Germany

Robert F.H. Fischer
Institut für Nachrichtentechnik, Universität Ulm, Germany

6. References

[1] Divsalar, D. & Simon, M. K. [1990]. Multiple-Symbol Differential Detection of *MPSK*, *IEEE Trans. Commun.* 38(3): 300–308.

[2] Farhang, M. & Salehi, J. A. [2010]. Optimum Receiver Design for Transmitted-Reference Signaling, *IEEE Trans. Commun.* 58(5): 1589–1598.

[3] Guo, N. & Qiu, R. C. [2006]. Improved Autocorrelation Demodulation Receivers Based on Multiple-Symbol Detection for UWB Communications, *IEEE Trans. Wireless Commun.* 5(8): 2026–2031.

[4] *IEEE Std 802.15.4a-2007, IEEE Standard for PART 15.4: Wireless MAC and PHY Specifications for Low-Rate Wireless Personal Area Networks* [2007].

[5] Leib, H. & Pasupathy, S. [1988]. The Phase of a Vector Perturbed by Gaussian Noise and Differentially Coherent Receivers, *IEEE Trans. Inf. Theory* 34(6): 1491–1501.

[6] Lottici, V. & Tian, Z. [2008]. Multiple Symbol Differential Detection for UWB Communications, *IEEE Trans. Wireless Commun.* 7(5): 1656–1666.

[7] Molisch, A. F., Cassioli, D., Chong, C.-C., Emami, S., Fort, A., Kannan, B., Karedal, J., Kunisch, J., Schantz, H. G., Siwiak, K. & Win, M. Z. [2006]. A Comprehensive Standardized Model for Ultrawideband Propagation Channels, *IEEE Trans. Antennas Propag.* 54(11): 3151–3166.

[8] Molisch, A. F., Foerster, J. R. & Pendergrass, M. [2003]. Channel Models for Ultrawideband Personal Area Networks, *IEEE Wireless Commun. Mag.* 10(6): 14–21.

[9] Pausini, M. & Janssen, G. J. M. [2007]. Performance Analysis of UWB Autocorrelation Receivers Over Nakagami-Fading Channels, *IEEE J. Sel. Topics Signal Process.* 1(3): 443–455.

[10] Quek, T., Win, M. Z. & Dardari, D. [2007]. Unified Analysis of UWB Transmitted-Reference Schemes in the Presence of Narrowband Interference, *IEEE Trans. Wireless Commun.* 6(6): 2126–2139.

[11] Schenk, A. & Fischer, R. F. H. [2010a]. Multiple-Symbol-Detection-Based Noncoherent Receivers for Impulse-Radio Ultra-Wideband, *2010 International Zürich Seminar on Communications (IZS)*, Zürich, Switzerland, pp. 70–73.

[12] Schenk, A. & Fischer, R. F. H. [2010b]. Soft-Output Sphere Decoder for Multiple-Symbol Differential Detection of Impulse-Radio Ultra-Wideband, *2010 IEEE International Symposium on Information Theory (ISIT)*, Austin (TX), U.S.A., pp. 2258–2262.

[13] Schenk, A. & Fischer, R. F. H. [2011a]. Capacity of BICM Using (Bi-)Orthogonal Signal Constellations in the Wideband Regime, *2011 IEEE International Conference on Ultra-Wideband (ICUWB)*, Bologna, Italy.

[14] Schenk, A. & Fischer, R. F. H. [2011b]. Compressed-Sensing (Decision-Feedback) Differential Detection in Impulse-Radio Ultra-Wideband Systems, *2011 IEEE International Conference on Ultra-Wideband (ICUWB)*, Bologna, Italy.

[15] Schenk, A. & Fischer, R. F. H. [2011c]. Decision-Feedback Differential Detection in Impulse-Radio Ultra-Wideband Systems, *IEEE Trans. Commun.* 59(6): 1604–1611.

[16] Schenk, A. & Fischer, R. F. H. [2011d]. Design Rules for Bit-Interleaved Coded Impulse-Radio Ultra-Wideband Modulation with Autocorrelation-Based Detection, *2011 International Symposium on Wireless Communication Systems (ISWCS)*, Aachen, Germany, pp. 146–150.

[17] Schenk, A. & Fischer, R. F. H. [2012]. Low-Complexity Soft-Output Detection for Impulse-Radio Ultra-Wideband Systems Via Combining Multiple Observations, *2012 International Zürich Seminar on Communications (IZS)*, Zurich, Switzerland, pp. 119–122.

[18] Schenk, A., Fischer, R. F. H. & Lampe, L. [2009a]. A New Stopping Criterion for the Sphere Decoder in UWB Impulse-Radio Multiple-Symbol Differential Detection, *2009 IEEE International Conference on Ultra-Wideband (ICUWB)*, Vancouver, Canada, pp. 606–611.

[19] Schenk, A., Fischer, R. F. H. & Lampe, L. [2009b]. A Stopping Radius for the Sphere Decoder and its Application to MSDD of DPSK, *IEEE Commun. Lett.* 13(7): 465–467.

[20] Stark, W. [1985]. Capacity and Cutoff Rate of Noncoherent FSK with Nonselective Rician Fading, *IEEE Trans. Commun.* 33(11): 1153 – 1159.

[21] Studer, C., Burg, A. & Boelcskei, H. [2008]. Soft-Output Sphere Decoding: Algorithms and VLSI Implementation, *IEEE J. Sel. Areas Commun.* 26(2): 290–300.

[22] Wachsmann, U., Fischer, R. F. H. & Huber, J. B. [1999]. Multilevel Codes: Theoretical Concepts and Practical Design Rules, *IEEE Trans. Inf. Theory* 45(5): 1361–1391.

[23] Witrisal, K., Leus, G., Janssen, G., Pausini, M., Troesch, F., Zasowski, T. & Romme, J. [2009]. Noncoherent Ultra-Wideband Systems, *IEEE Signal Process. Mag.* 26(4): 48–66.

[24] Zhongmin W., Arce, G. R., Paredes, J. L. & Sadler, B. M. [2007]. Compressed Detection for Ultra-Wideband Impulse Radio, *2007 IEEE 8th Workshop Signal Processing Advances in Wireless Communications (SPAWC)*, pp. 1–5.